The Chemistry of Boron Nitride Nanotubes (BNNTs) and PC-BNNT Composites: Towards Transparent Armour Applications

Guan, J. W.[1*], Derdouri, A.[2], Ashrafi B.[3], Patenaude, E.[2], Martinez-Rubi, Y.[1], Jakubinek M. B.[1], Shin, H.[1], Kim, K. S.[1], Kingston, T. C.[1], Simard B.[1]

[1] Security and Disruptive Technology Portfolio, National Research Council Canada, Ottawa, ON, K1A 0R6, Canada

[2] Automotive and Surface Transportation Portfolio, National Research Council Canada, Boucherville, QC, J4B 6Y4, Canada

[3] Aerospace Portfolio, National Research Council Canada, Montreal, QC H3T 2B2, Canada

* Corresponding author (Jingwen.guan@nrc-cnrc.gc.ca)

Keywords: *BNNTs, polycarbonate composites, mechanical property*

ABSTRACT

Boron nitride nanotubes (BNNTs) possess excellent mechanical properties due to their unique structural architectures and are the favorable candidates for fabricating nano-based composite materials. Along with high thermal stability, high neutron absorption capacity and other desirable features, BNNTs have no absorptions in the visible range, making them ideal candidates for transparent material application including as reinforcement nano-filler in transparent polymeric nanocomposites. The recent advances in BNNT production are making sufficient quantities available for composites development. In this study, we will discuss preliminary results related to the integration of BNNTs into a polycarbonate matrix (PC). Two different fabrication methods of tensile specimens were employed. The first method was by hot-pressing powder samples into thin films of about 200 μm in thickness followed by punching dog-bone specimens using a die punch. The second method was by melt-mixing using a twin-screw micro-extruder followed by hot-compression molding to make plaques, and tensile bars were punched. The initial target is to gain mechanical improvements by tuning the chemistry, integration and material processing before aiming at high transparency BNNT-PC composites.

1 INTRODUCTION

Recent breakthroughs in large quantity synthesis of BNNT using an industrially scalable induction thermal plasma process developed at the National Research Council Canada (NRC) have accelerated the research and development of chemistry, assembly, composites and applications toward multifunctional engineering materials based on BNNTs. The NRC-produced, highly crystalline BNNTs have few-walls, small-diameters (~5 nm) and micrometer-scales length. At a production rate now 30 g/h, 200 g of raw BNNT have been harvested from a single run with a standard protocol [1, 2].

BNNTs exhibit various properties similar to their carbon nanotube (CNTs) counterparts, such as comparable mechanical properties and thermal conductivity [3-5], but have substantially higher thermal stability (stable ≥ 800 ^{o}C in air) [6], a larger band gap of ~ 5 eV [7] and transparency in the visible region that provides advantages for

transparent composite armors. These unique characteristics make BNNTs very attractive in research and industrial development of higher performance, light-weight and stronger polymer composites that offer potential to impact various multifunctional engineering structural materials in aerospace and armor industries. Similar to CNTs, BNNTs also tend to bundle together forming ropes or clumps that are not effectively dispersed in a matrix and therefore have poor interface interactions. However, unlike CNTs, the high polarization of B-N bonds could make their chemistry in some cases different from CNTs, and there are limited reports on chemistry of BNNTs [8-13]. Hence, chemical surface modifications, especially, with desired surface functional groups compatible with a target matrix become crucial in the development of BNNT-polymer composites. The dispersibility and filler-matrix interface obtained through surface modifications will also be critical to take advantages of BNNTs transparency in the visible light region for applications like transparent armour. In this study, we focused on BNNT-PC composite, and much attention was paid to the interface compatibility and dispersion. The initially mechanical performances by minimal surface chemical modifications of BNNTs were studied in the course toward applications.

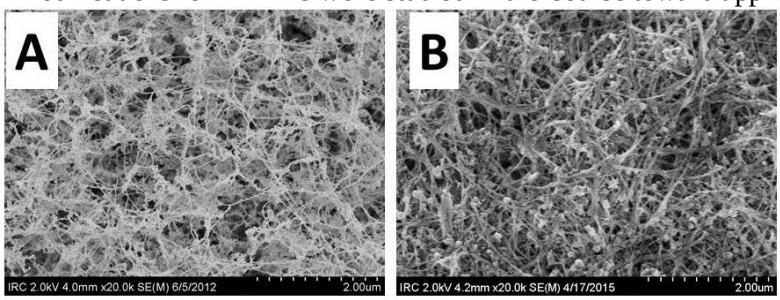

Figure 1. SEM images of raw BNNTs (A) and BNNTs purified to a certain degree (B).

2 MATERIALS AND PROCESSING

2.1 Synthesis and purification of BNNTs

An industrially scalable plasma process was used for the continuous production of highly crystalline, small-diameter (~ 5 nm) BNNTs [1, 2]. The raw BNNTs, shown in Fig. 1A, contain impurities such as unreacted feedstock h-BN powder particles, new h-BN particles and amorphous BN flakes, organic BN species, polyborazine-like BN polymers, and variety of elemental boron particles. These impurities affect the chemistry on BNNTs and BNNT-reinforced polymer composites by altering the actual BNNT-polymer interaction and filler composition. Reducing or eliminating these impurities in as-produced BNNT material is essential for the study of BNNT reinforcement effect. We have developed an in-house protocol that involves different solvent extractions with sonication followed by either processing the pre-purified BNNT in bromine aqueous solution or baking in air to removed most of the elemental B particles as shown in Fig. 1B.

2.2 Chemistry on BNNT tubes

In order to have a better loading transfer and a good interface interaction between BNNTs and matrix, debundling by surface chemical modification with compatible functional groups becomes desirable. Although the large band gap (~ 5eV) electronic structure of BNNTs implies that they may have totally different chemical reactive mechanisms than CNTs, we attempted to use a similar chemistry on BNNTs to verify whether the same approach results in the same functionality or different product. As we have recently reported, BNNTs negatively charged through electron transfer from sodium naphthalide can readily carry out a nucleophilic attack on hexyl bromide and covalently form alkyl-functionalized BNNTs as shown in Fig. 2 [12].

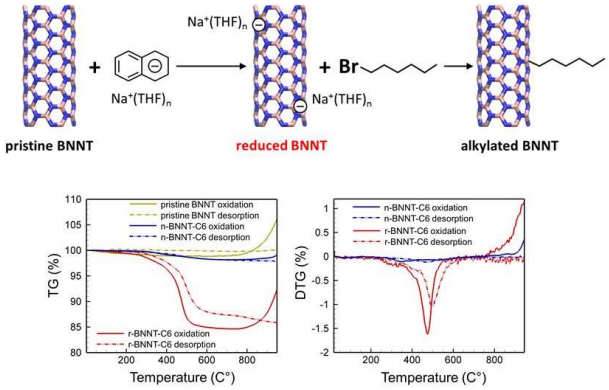

Figure 2. Schematic illustration of the reduction chemistry on BNNTs followed by nucleophilic reaction (top); TGA analysis where the significant weight loss above 400 ^{o}C(bottom) [Ref. 12]

This result has indicated that the chemistry on BNNTs may be similar to their CNTs counterparts with certain reactions, such as for this reduced nanotube chemistry. To serve our purpose for making BNNT-PC composites with good interfaces, we targeted hydroxyl (–OH) and/or amino (-NH_2) functional groups that anchor to the surfaces of BNNTs. There are many ways that may covalently attach such functional groups to BNNT surfaces. In this study, we discovered that in the step of removing elemental boron from the pre-purified BNNTs in a aqueous solution of bromine, not only were the enriched elemental boron particles effectively removed, but BNNTs were also functionalized with –OH and –NH_2 functional groups, most likely, by generating cavities on the surfaces of BNNTs as schematically illustrated in Fig. 3.

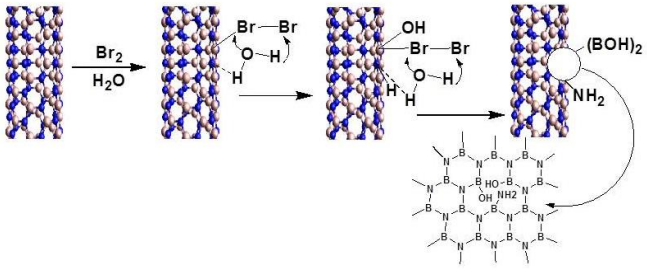

Figure 3. Proposed mechanism of –OH/-NH_2 surface functional group generation of BNNT treated with bromine.

The bromine-treated BNNTs were further analyzed with thermogravimetric analysis (TGA) and in-line FTIR spectroscopy, wherein we observed two desorption peaks at about 120 ^{o}C and 220 ^{o}C. The first peak at 120 ^{o}C was mainly from adsorbed water, and the second peak at 220 ^{o}C contained a mixture of water and ammonia, which consistent with decomposition of the –OH and –NH_2 groups on BNNT surfaces.

2.3 BNNT-PC Composite Material Preparation

In this study, the -OH/NH_2 functionalized BNNTs through bromine aqueous solution treatment and the commercial polycarbonate Lexan PC Resin 141R-112 were used for composite production. A typical BNNT-PC composite sample preparation with different BNNT loading was carried out in the following example: 35 g PC was dissolved in 450 ml of chloroform, and 1.46 g BNNT (for 4 wt% loading) was dispersed in 150 ml DMF by bath-sonication. After stirring for 2 hrs, the BNNT suspension in DMF was bath-sonicated for 30 min and stirred overnight, and then

bath-sonicated for another 30 min. To the well-dispersed BNNT-DMF suspension, 100 ml of PC solution was dropwise added under vigorous magnetic stirring. After addition the mixture was bath-sonicated for 20 min, and then poured into the rest of the PC chloroform solution. The temporarily two-layered mixtures were mixed quickly by shaking and magnetic stirring, and the mixture became hot for a couple minutes. The liquid mixture suspension was stirred at room temperature overnight. During which time it became very viscous and finally a solid gel as shown in Fig. 4. The gel was dried in a vacuum oven to remove the solvents and the solid sample was further dried up to 220 ^{o}C overnight and then cooled to room temperature under argon.

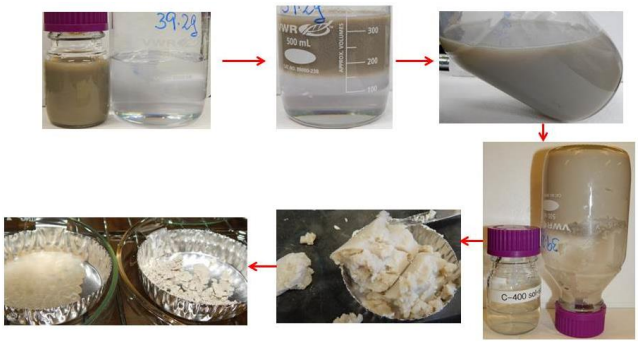

Figure 4. BNNT-PC composite preparation process and observations.

2.4 DSC analysis of the powder BNNT-PC composite

A powder sample and a sample melt-processed by micro-extrusion were analyzed by differential scanning calorimetry (DSC). The first DSC curves shown in Fig. 5 display an endothermic peak at about 233 ^{o}C for all three powder samples and a glass transition temperature (T_g) around 145 ^{o}C. However, during the second run no endotherm peak is observed while T_g remains unchanged. The endothermic peak at 233 ^{o}C might be explained as by fusion of some PC crystalline structure caused by BNNTs during solvent removal and, once the sample goes through a heating process as during the first heating in a DSC run or as in melting extrusion, the PC crystalline structure is destroyed and the PC matrix recovers its amorphous state.

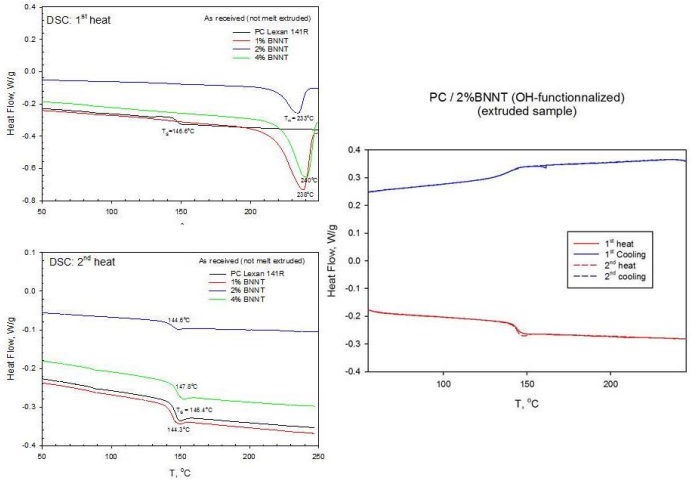

Figure **5**. DSC analyses of BNNT-PC composites before and after the melt extrusion.

2.5 *Analysis of WAXD vs* DSC

As shown in Table 1 the wide-angle X-ray diffraction (WAXD) analysis offers a quantitative validation for the crystalline content of the BNNT-PC samples before and after melting, which further confirms and is consisted with the results from the DSC analysis.

χ_c, %	PC Lexan 141		PC/BNNT-OH 1%		PC/BNNT-OH 2%		PC/BNNT-OH 4%	
	powder	Melt processed	powder	Melt processed	powder	Melt processed	powder	Melt processed
DSC	Amorphous		31.2	Amorphous	26.3	amorphous	29.4	Amorphous
WAXD	Amorphous		33.0	Amorphous	N/M	N/M	37.4	Amorphous

Table 1. DSC and WAXD analysis of crystallinity of neat PC and BNNT-PC composite before and after melt extrusion.

2.6 Thin-film process by hot-press

The dry powder of BNNT-PC composite was poured inside an open mold to produce films of 200 µm in thickness and 5 cm in diameter. Kapton films were used on both sides to facilitate specimen removal. Stepwise pressing at elevated temperature was employed to avoid air bubbles trapped in the specimen. Conditions were a starting at temperature of 150 °C, maximum temperature of 240 °C and maximum pressure of 15000 pounds. Temperature steps included: 150 °C, 175 °C, 200 °C, 220 °C and 240 °C. A ramp rate of 15 °C/min and a holding time of 5-8 minutes at each temperature stage were selected. The pressed sample was cooled to room temperature using compressed air. The compression-molded thin films, as shown in Fig. 6, were ready to be punched to fabricate small tensile coupons for mechanical tests and demonstrated good transparency up to 4 wt% BNNT loading.

Figure **6**. Optical transparency comparison of thin-films with 0, 2 and 4 wt% BNNT loading.

2.7 Tensile tests of thin-films

A micro-tensile test frame (Fullam Substage Test Frame) was used to measure the mechanical properties of the fabricated thin films. At least five dogbone specimens, according to ISO 527-2 (Type 1BB), were tested. For all tests a displacement rate of 1 mm/min was used. As reported in Table 2, the highest Young's modulus is for the nanocomposite containing 4 wt% of OH-functionalized BNNTs (31% increase versus neat PC). For all nanocomposites, tensile stress at maximum load increased by up to 20%. On the other hand, stress at failure essentially remained unchanged while strain at failure was significantly reduced in comparison to the neat PC. This reduction was more pronounced for specimens containing OH-functionalized BNNTs.

	Young's Modulus (MPa)	Tensile stress @ Max load (MPa)	Tensile strain @ Max load (%)	Tensile stress @break (MPa)	Tensile strain @ break (%)
PC-141R	1740±170	44.6±8.1	4.90±0.13	42.1±3.9	60±41
BNNT-OH 1 wt%	1960±60	50.1±1.5	5.12±0.31	43.6±2.4	15±10
BNNT-OH 4 wt%	2280±200	51.0±1.6	4.73±0.23	42.4±6.6	4±2

Table 2. Comparisons of mechanical properties of functionalized BNNT-PC composites with neat PC.

.

2.8 Melt-mixing of the BNNT-PC powder samples and pelletizing

PC/BNNT powder at BNNT concentrations of 1%, 2% and 4% and pure PC Lexan 141R powder were first dried overnight under vacuum at 110 ^{o}C. The melt-mixing was then carried out at 250 ^{o}C using a Thermo Haake MiniLab conical twin screw co-rotating extruder (5g max capacity). To improve the nanotube dispersion within the PC matrix the melt was allowed to recirculate for 3 min within the barrel/screw system by controlling a valve at the end of the screws. The rotational screws speed was fixed at 100 RPM. At the end of the 3 min mixing period the valve was opened and the composite was melt-extruded through a rectangular die, cooled and pelletized into small pieces. Figure 7 shows images of the mini twin screw extruder used. For each BNNT concentration about 40g of nanocomposite was prepared. Pellets of PC Lexan 141R were also prepared under the same conditions to match the processing history of the nanocomposites.

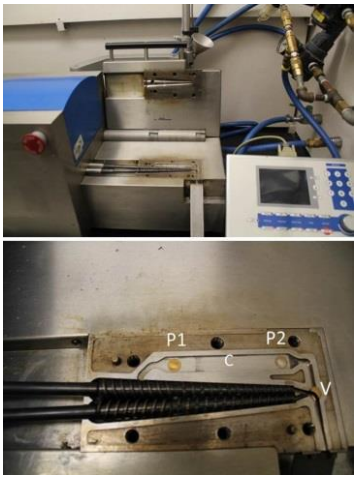

Figure **7. Top:** Twin screw extruder (open view) showing the conical screw configuration; Bottom: A close-up indicating the position of the recirculation channel (C), exit valve (V) and two pressure transducers (P1 and P2).

2.9 Compression molding of samples, standard ASTM specimen preparations and tensile tests

Part of the collected material was used to make 1.2 mm thick rectangular plaques (10 x 12 cm) by compression molding using a Carver hot press. The pellets were preheated at 230 ^{o}C for 2 min under no pressure within the rectangular cavity of the mold and compressed for 0.5 min under 1T (tonf/in^2 = 138 bars), then 2T for 0.5 min and

finally under 5T for 1 min. Cooling under 5T was then carried out down to 75°C before demolding the plaques. Four ASTM type IV tensile bars for tensile testing were cut by a water jet technique from the compression molded plaques.

Tensile properties of the pristine PC and BNNT/PC nanocomposites were determined following ASTM D638 protocol using compression molded type IV tensile bars (gauge length and width of 25 mm and 6.0 mm respectively), a load cell of 5 kN, and speed of 5 mm/min at room temperature (23 ℃). Four tensile bars were tested and the results averaged (Table 3). The tensile modulus increased only slightly when the BNNT concentration was at 2% and 4%, by ~13% with respect to pure PC (for both samples), while the tensile stress at yield and maximum load remained about constant or slightly decreased for the highest BNNT concentrations. The stress and elongation at break were less consistent as they are more prone to experimental error. The lack of substantial improvement in the tensile strength or modulus is most probably due to the lack of a good dispersion of the BNNTs and/or strong adhesion with the PC matrix.

	Tensile stress @Max load (MPa)	Tensile strain @ Max load (%)	Young's Modulus (MPa)	Tensile stress @Yield (0.2% offset), (MPa)	Tensile strain @break (%)	Tensile stress @break (MPa)	Energy @break (J)
PC-141R	67.6 (0.6)	6.4 (0.8)	2405 (94)	39.6 (2)	76.2 (26)	50.1 (2.6)	7.12 (2.4)
PC/BNNT1%	68.2 (0.4)	7.0 (0.2)	2435 (141)	39.6 (2.5)	101 (62)	55.8 (7)	9.5 (5.9)
% diff.	+0.9	+9	+1.2	0	+32	+11.4	33
PC/BNNT2%	65.6 (0.1)	5.7 (0.2)	2730 (207)	36.3 (1.8)	10.6 (4.2)	13.9 (14.1)	0.73 (0.2)
% diff.	-2.9	-11	+13.5	-8	-86	-72	-90
PC/BNNT4%	61.6 (11)	4.4 (1.7)	2705 (51)	42.3 (1.5)	11.3 (8)	49.7 (2.9)	1.0 (0.8)
% diff.	-7.4	-31	+12.5	+6.8	-85	-1	-86

Table 3. Summary of tensile properties of neat PC, and of 1, 2 and 4 wt% BNNT-PC nanocomposites melt-mixed by twin-screw extrusion. Standard deviations are indicated in parenthesis.

2.10 SEM and TEM analysis of BNNT dispersion in the composites

To have a better understanding of the mechanical performance with different BNNT loadings and their inconsistencies, the standard specimens were further investigated for their surface morphology and interface interactions and dispersity of BNNTs in the PC matrix with SEM and TEM. As shown from cryo-fractured surfaces of the micro-extruded BNNT-PC sample at 4 wt% by SEM (Figure 8) there were obvious aggregations of BNNTs within the PC matrix. These randomly allocated micro-aggregations inside the specimens could be the main factor to cause the fluctuation of the data. However, from TEM analysis we also observed a lots of individualized BNNTs nicely dispersed in PC matrix (Figure 9), which attributed to the marginal improvement of the mechanical properties, indicating that further efforts need to reduce the number of aggregations of BNNTs and increase of individual tubes within the PC matrix. It

seems that all these individual tubes are aligned to the same direction. This alignment may be due to shear flow during the extrusion process or could possibly result from the TEM sample preparation.

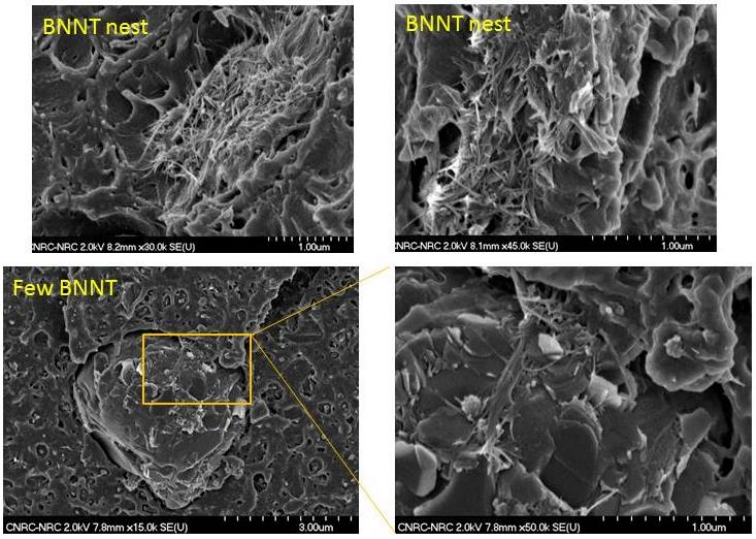

Figure 8. SEM images on cryo-fractured surface of micro-extruded BNNT-PC at 4 wt% loading

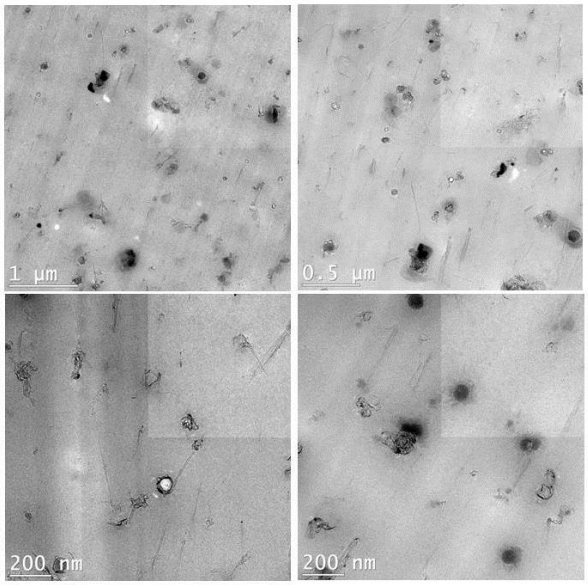

Figure 9. TEM images of micro-extruded BNNT-PC at 4 wt% loading.

As the BNNT sample used was only purified to certain level of purity, there were still many blocks and onion-like shelled structures remaining in the sample. It was not surprising that we have observed these particles from the TEM images shown in Figure 9. These particle impurities might impact the actual performance of the composites and it is expected that the BNNTs with a higher degree of purity and a better individualization of BNNTs within the PC matrix may yield a better mechanical performance.

3 DISCUSSIONS AND CONCLUSIONS

In this study we processed the same BNNT-PC composite materials in two different processes. The first was to hot-press a powder sample within an open round metal shim into around 200 µm thickness thin-films. The second was to extrude the powder composite sample using a micro-extruder followed by compression molding the extruded pellets into standard dogbones. The former process is fast and needs only small samples to make tensile specimens. The latter process needs to have a large size of sample to make sufficient standard specimens (usually over 30 g composite for each sample) and is a longer process. Although the specimens from these two different processes had quite different performances such as for their Young's modulus shown in Fig. 10, the extruded samples had higher Young's modulus than the thin film samples; meanwhile, the extruded neat PC also gave high values with small variation. However, both data sets showed the same trend of Young's modulus enhancement with the increase of BNNT loadings.

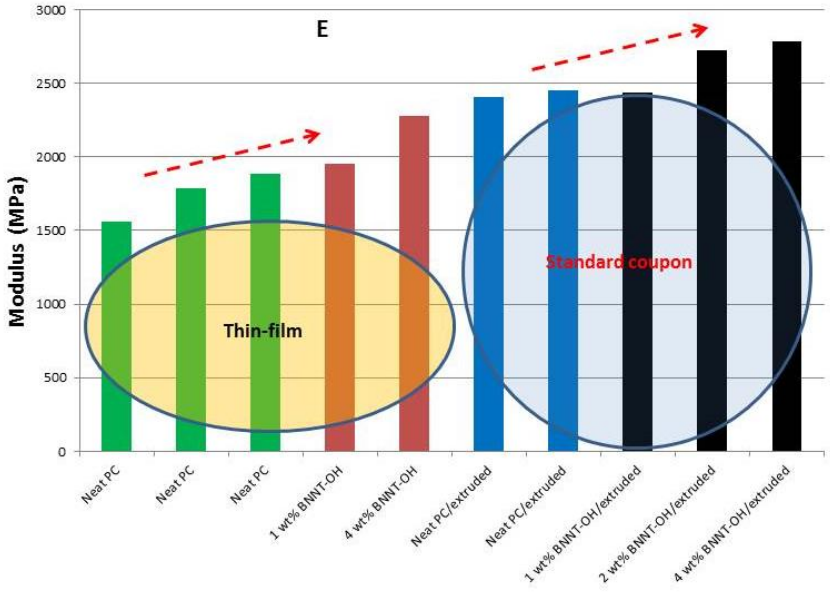

Figure 10. Comparison of Young's modulus from thin-films and extruded samples.

There may have been more fluctuation from one time to another, even for the neat PC specimens, from the thin-film process than from the micro-extruding process. The causes of the differences can be resulted from many factors such as a better mixing, more individualized tubes, errors from specimen preparations, and the accuracy of micro-stage tester to the standard dogbone tester. Nevertheless, the enhancement of Young's modulus seems to have the same trend with the increase of BNNT loading as indicated by the dotted arrows in Figure 10. The 200 µm thin-films showed quite good optical transparency even at 4 wt% BNNT loading indicating a high potential for the development of transparent coating and armour with BNNT reinforcement. As we have seen from the purity of BNNT used and the SEM morphology analysis, there was still a significant amount of impurity particles that could not only affect the mechanical performance but also affect the optical transparency. The future work is relying on highly purified BNNTs and surface modifications by covalently anchoring desired surface functional groups for a better compatibility with the polycarbonate matrix.

4 REFERENCES

[1] K. S. Kim, Ch. T. Kingston, A. Hrdina, M. B. Jakubinek, J. W. Guan, M. Plunkett and B. Simard. "Hydrogen-catalyzed, pilot-scale production of small-diameter boron nitride nanotubes and their macroscopic assemblies". *ACS Nano*, Vol. 8, No. 6, pp 6211-6220, 2014.

[2] K. S. Kim, Ch. T. Kingston and B. Simard. "*Boron nitride nanotubes and process for production thereof*". PCT WO2014/169382.

[3] D. Golberg, Y. Bando, Y. Hang, T. Terao, M. Mitome, C. Tang and C. Zhi. "Boron nitride nanotubes and nanosheets". *ACS Nano*., Vol.4, pp 2979-2993, 2010.

[4] C. Zhi, Y. Bando, C. C. Tang and D. Golberg. "Boron nitride nanotubes". *Mater. Sci. Eng. Res.*" Vol. 70, pp 92-111, 2010.

[5] M. J. Jakubinek, J. F. Niven, M. B. Johnson, B. Ashrafi, K. S. Kim, B. Simard and M. A. White. "Thermal conductivity of bulk boron nitride nanotube sheets and their epoxy-impregnated composites". *Phys. Status Solidi A*, Vol. 213, No. 8, pp 2237-2242, 2016.

[6] Y. Chen, J. Zou, S. J Campbell and G. Le Caer. "Boron nitride nanotubes: pronounced resistance to oxidation". *Appl. Phys. Lett.*, Vol. 84, pp 2430-2432, 2004.

[7] A. Rubio,J. L. Corkill and M. L. Cohen. "Theory of graphitic boron nitride nanotubes" *Phys. Rev. B*, Vol. 49, No. 7, pp 5081-5084, 1994.

[8] S. M. Nakhmanson, A. Calzolari, V. Meunier, J. Bernholc and M. Buongiorno Nardelli. "Spontaneous polarization and piezoelectricity in boron nitride nanotubes" *Phys. Rev. B*, Vol. 67, pp 235406, 2003.

[9] Q. Weng, X. Wang, X. Wang, Y. Bando and D. Golberg. "Functionalized hexagonal boron nitride nanomaterials: emerging properties and applications". *Chem. Soc. Rev.*, Vol. 45, pp 3989-4012, 2016.

[10] D. Kim, H. Muramatsu and Y. A. Kim. "Hydrolytic unzipping of boron nitride nanotubes in nitric acid". *Nanoscale Res. Lett.*, 2017. DOI: 10.1186/s11671-017-1877-3

[11] S. Mukhopadhyay, R. H. Scheicher, R. Pandey and S. P. Karna. "Sensitivity of boron nitride nanotubes toward biomolecules of different polarities". *J. Phys. Chem. Lett.*, Vol. 2, pp 2442-2447, 2011.

[12] H. Shin, J. W. Guan, M. Z. Zgierski, K. S. Kim, Ch. T. Kingston and B. Simard. "Covalent functionalization of boron nitride nanotubes via reduction chemistry". *ACS Nano*, Vol. 9, No. 12, pp 12573-12582, 2015.

[13] D. Kim, S. Nakajima, T. Sawada, M. Iwasaki, S. Kawauchi, C. Zhi, Y. Bando, D. Golberg and T. Serizawa. "Sonication-assisted alcoholysis of boron nitride nanotubes for their sidewalls chemical peeling". *Chem. Commun.*, Vol. 51, pp 7104-7107, 2015.